Exact solution for the critical state in thin superconductor strips with field-dependent or anisotropic pinning

Grigorii P. Mikitik
B. Verkin Institute for Low Temperature Physics & Engineering, National Ukrainian Academy of Sciences, Kharkov 310164, Ukraine

Ernst Helmut Brandt
Max-Planck-Institut für Metallforschung, D-70506 Stuttgart, Germany
(Received 14 January 2000; revised manuscript received 10 April 2000)

An exact analytical solution is given for the critical state problem in long thin type-II superconductor strips in a perpendicular magnetic field for the case when the critical current density $j_c(B)$ depends on the local induction B according to a simple three-parameter model. This model describes both isotropic superconductors with this $j_c(B)$ dependence, but also superconductors with anisotropic pinning with a dependence $j_c(\theta)$ where θ is the tilt angle of the flux lines away from the normal to the specimen plane.

I. INTRODUCTION

The critical state model[1] for the magnetic behavior of superconductors with flux-line pinning has proven very useful[2] though it originally was applied to the simple (demagnetization-free) *longitudinal* geometry of long superconductors in parallel magnetic field. It took over 30 years until an analytical solution of the critical state model was obtained for the more realistic *transverse* geometry of thin superconductors. The solutions were derived for thin disks[3] and strips[4] in a perpendicular magnetic field, extending an earlier work on superconductor strips with transport current,[5] and finally for elliptic-shaped platelets.[6] Recent detailed numerical work for strips[7] and disks[8] of finite thickness shows how the transition from longitudinal to transverse geometry occurs with changing aspect ratio of the specimen.

So far, in the transverse geometry all analytical solutions of the critical state model were restricted to the Bean model of constant critical current density $j_c = \text{const}$, but in many experiments $j_c = j_c(B)$ depends on the local magnetic induction B. For example, the simple Kim model[9] $j_c(B) = j_c(0)/(1+|B|/B_0)$ was considered in many experimental and theoretical papers, see, e.g., the reviews of Refs. 2,10 and 11 and the partly analytical calculations for thin strips[12] and disks.[13] While numerical computations easily allow us to consider any $j_c(B)$ dependence,[7,8,11,14] an exact analytical solution of some model may give deeper insight since it yields explicit dependences of the resulting quantities on the input parameters.

In the highly anisotropic high-T_c superconductors the flux-line pinning in general depends on the angle θ between the local direction of the magnetic induction **B** and the c axis, which in typical experiments is normal to the plane of the sample. For example, this type of anisotropy occurs when one takes into account the intrinsic pinning exerted by the CuO planes or the pinning by extended defects.[11] It has been shown recently[15–18] that for thin superconductors of any shape (with thickness d much smaller than the lateral extension L but larger than the magnetic penetration depth λ) any such out-of-plane anisotropy of pinning is equivalent to an induction dependence of the critical sheet current $J_c(B)$ (the sheet current is defined as the current density integrated over the film thickness). Thus the description of the two-dimensional critical state, e.g., in an anisotropic strip, can be reduced to the analysis of a one-dimensional problem with some $J_c(B)$. In this case the characteristic scale B_0 over which $J_c(B)$ changes is of the order of $\mu_0 j_c d$.

In this paper we present a simple model which allows for an analytical solution to the critical state in thin superconductor strips in perpendicular field with field-dependent critical current density $j_c(B)$ or, equivalently, with anisotropic pinning described by a $j_c(\theta)$. Our three-parameter model $j_c(B)$ consists of two straight lines, an inclined line at small B and a horizontal line at larger B. This simple but rather general model is equivalent to a piecewise constant angular dependence $j_c(\theta) = j_{c1}$ for $0 \leqslant \theta < \theta_0$ and $j_c(\theta) = j_{c2}$ for $\theta_0 \leqslant \theta < \pi/2$ where j_{c1}, j_{c2}, and θ_0 are the parameters of the model. This angular dependence allows to model both the intrinsic pinning by the CuO planes and the pinning by columnar defects in high-T_c superconductors. Its exact analytical solution points out features which distinguish the critical states in isotropic and anisotropic superconductors and it allows us to estimate the type and parameters of anisotropy of flux-line pinning in real superconducting samples. We find below that the steepness of the flux front in the superconductor strongly depends on the anisotropy of pinning. In particular, in the case corresponding to the intrinsic pinning in high-T_c superconductors, the front is a very sharp step, which should be taken into account in analyzing data of local magnetic measurements. We shall show that under certain conditions *two penetrating flux fronts* can occur in an anisotropic superconductor.

As usual, we consider here the cases when the characteristic magnetic field in the sample is sufficiently large such that the difference between the magnetic induction B and the field H may be disregarded. This condition is satisfied when $j_c d$ is much larger than the lower critical field H_{c1} (otherwise, the so-called geometric barrier[19] must be taken into account). We shall thus express all the following equations in terms of the magnetic field H, related to the current density by the Maxwell equation $\mathbf{j} = \nabla \times \mathbf{H}$.

II. MODEL AND ITS SOLUTION

We consider an infinitely long strip of width $2w$ and thickness d, filling the space $-w \leqslant x \leqslant w$, $-d/2 \leqslant z \leqslant d/2$, i.e., we place the y axis of the coordinate system along the central line of the strip and the z axis along the external magnetic field H_a which is applied normal to the plane of the strip. The increasing applied field induces a sheet current J along y, which is related to the z component of the magnetic field in the plane $z=0$ by the Biot-Savart law,

$$H_z(x) = H_a + \frac{1}{2\pi}\int_{-w}^{w} \frac{J(t)dt}{t-x}. \tag{1}$$

Here and below all singular integrals are taken in the sense of the Cauchy principal value. The penetration of the magnetic flux into the superconducting strip is described by the following critical state equations: In the flux-free central region $|x| \leqslant b(H_a)$ one has

$$H_z = 0, \tag{2}$$

while in the region $b(H_a) \leqslant |x| \leqslant w$, where the flux already exists, one has

$$|J(x)| = J_c[H_z(x)]. \tag{3}$$

The position $x=b(H_a)$ of the boundary separating the regions, is found by solving these equations. In Eq. (3) $J_c(H_z)$ is the critical value of the sheet current. At present an exact solution of Eqs. (1)–(3) is known[4,20,21] only for the Bean critical state model where $J_c = \text{const}$. Below we shall obtain the exact solution for the more general case when $J_c(|H_z|)$ has the model form (see Fig. 1):

$$J_c(H_z) = J_{c1} - \gamma H_z \quad \text{for} \quad 0 \leqslant H_z \leqslant H_z^0,$$

$$J_c(H_z) = J_{c0} \quad \text{for} \quad H_z \geqslant H_z^0. \tag{4}$$

Here $\gamma = (J_{c1} - J_{c0})/H_z^0$; the three parameters J_{c1}, J_{c0}, and H_z^0 may have any positive value.

In the case of anisotropic pinning the critical current density j_c depends on the angle θ between the local direction of the magnetic induction and the normal to the strip plane (i.e., the c axis). Since in the partly penetrated critical state the flux lines are always curved, this anisotropy means that j_c depends on the coordinate z across the thickness of the strip. Therefore the critical state problem becomes two-dimensional (2D) in *thin anisotropic* samples. However, as was shown in Ref. 18, the smallness of the parameter d/w enables one to split the 2D problem into two one-dimensional problems: The first one treats the critical state across the thickness of the strip and can be solved in general form; its solution leads to a relation between the critical sheet current J_c and H_z (H_z is practically independent of z). The second problem treats the strip as infinitely thin and is described by Eqs. (1)–(3) with $J_c(H_z)$ obtained from the solution of the first problem. If j_c does not depend explicitly on the magnitude of the magnetic induction, the above-mentioned relationship can be presented in the form[18]

$$j_c(\theta)d = J_c(H_z) - H_z \frac{dJ_z(H_z)}{dH_z},$$

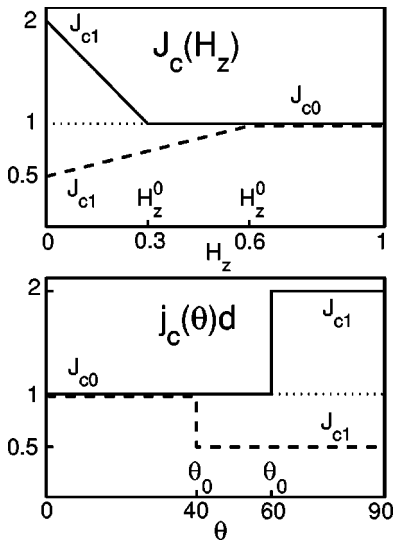

FIG. 1. Visualization of the dependence of the critical sheet current on the perpendicular magnetic field [$J_c(H_z)$, Eq. (4), upper plot], equivalent to an out-of-plane anisotropy [$j_c(\theta)$, Eq. (5), lower plot]. The model has three independent positive parameters, J_{c0}, J_{c1}, and H_z^0, all of same dimension. In this plot we put $J_{c0}=1$ and show two examples: $J_{c1}=2$ (intrinsic pining, solid lines) and $J_{c1}=0.5$ (dashed lines), with $H_z^0=0.3$ (0.6) equivalent to $\theta_0 = \arctan(J_{c0}/2H_z^0) \approx 60$ (40) degrees.

$$\tan(\theta) = \frac{J_c(H_z)}{2H_z}.$$

It is easy to verify that the function defined by Eqs. (4) yields the following θ dependence of the critical current density shown in Fig. 1:

$$j_c(\theta) = J_{c0}/d \quad \text{for} \quad 0 \leqslant \theta \leqslant \theta_0,$$

$$j_c(\theta) = J_{c1}/d \quad \text{for} \quad \theta_0 \leqslant \theta \leqslant \pi/2, \tag{5}$$

where $\tan\theta_0 = J_{c0}/2H_z^0$. Thus in the case under study we can say that the H_z dependence of J_c in Eq. (4) is due to the nonuniform distribution of j_c across the thickness of the sample, and the results obtained below correspond to the solution of the critical state problem with $j_c(\theta)$ given by Eqs. (5). It should be also noted that the *two-dimensional* solution of the critical state equations for the anisotropic strip of small but finite thickness can be found in analytical form by using these results and Eqs. (5), (6), and (9)–(11) of Ref. 18.

It is well known that in high-T_c superconductors the intrinsic pinning by the CuO planes[22] yields a peak in $j_c(\theta)$ at $\theta = \pi/2$, whereas the columnar defects normal to the film produce a peak at $\theta = 0$. In both these cases we shall approximate the angular dependences of j_c by Eqs. (5): the case $\gamma > 0$ models the intrinsic pinning and $\gamma < 0$ pinning by columnar defects, see Fig. 1. Although this model is a fairly rough approximation, it nevertheless takes into account the peaks in $j_c(\theta)$ and allows to understand some essential features of the critical state in anisotropic superconductors in terms of analytic results.

Accounting for the symmetry of the sheet current, $J(-x) = -J(x)$, we seek the solution of Eqs. (1)–(4) in the form

$$J(x)=-\frac{x}{|x|}[J_0(x)+J_1(x)], \tag{6}$$

where

$$J_0(x)=J_{c0}, \quad b^2\leqslant x^2\leqslant w^2, \tag{7}$$

$$J_0(x)=\frac{2J_{c0}}{\pi}\arctan\left[\frac{(w^2-b^2)x^2}{w^2(b^2-x^2)}\right]^{1/2}, \quad x^2\leqslant b^2, \tag{8}$$

while $J_1(x)$ is a new unknown function. The parameter b defines the position of the flux front, i.e., $x=b$ is the point where H_z goes to zero. This parameter depends on H_a and must be determined together with $J_1(x)$. Both $J_0(x)$ and $J_1(x)$ (and the magnetic field below) are even functions, which depend only on x^2. The function $J_0(x)$ has the form of the exact solution[4] to Eqs. (1)–(3) in the case when $J_c=J_{c0}$ and the external magnetic field is equal to

$$H_b=H_{cs}\,\mathrm{arccosh}(w/b),$$

where $H_{cs}=J_{c0}/\pi$. Using Eqs. (1) and (6)–(8), the expression for the magnetic field can be rewritten as

$$H_z(x)=H_0(x)-\frac{1}{2\pi}\int_0^{a^2}\frac{J_1(\sqrt{s})ds}{s-x^2}, \tag{9}$$

where a is defined by the equality $H_z(a)=H_z^0$, and $H_0(x)$ is the sum of H_a and the field generated by the current $J_0(x)$,[4]

$$H_0(x)=H_a-H_b, \quad 0\leqslant x^2\leqslant b^2, \tag{10}$$

$$H_0(x)=H_a-H_b+H_{cs}\,\mathrm{arctanh}\left[\frac{(x^2-b^2)w^2}{x^2(w^2-b^2)}\right]^{1/2},$$

$$b^2\leqslant x^2\leqslant w^2. \tag{11}$$

In Eq. (9) it was taken into account that $J_1(x)$ differs from zero only in the region $0\leqslant x^2\leqslant a^2$ where $H_z(x)<H_z^0$.

With the above formulas, the critical state equations take the following form: In the interval $0\leqslant x^2\leqslant b^2$ one has

$$H_0(x)=\frac{1}{2\pi}\int_0^{a^2}\frac{J_1(\sqrt{s})ds}{s-x^2}, \tag{12}$$

and in the region $b^2\leqslant x^2\leqslant a^2$ we arrive at

$$H_0(x)-H_z^0=-\frac{J_1(x)}{\gamma}+\frac{1}{2\pi}\int_0^{a^2}\frac{J_1(\sqrt{s})ds}{s-x^2}. \tag{13}$$

In deriving Eq. (13) we have expressed $H_z(x)$ for $b^2\leqslant x^2\leqslant a^2$ in terms of $J_1(x)$ using the equality

$$H_z(x)=H_z^0-\frac{J_1(x)}{\gamma} \tag{14}$$

that follows from formulas (3), (4), (6), and (7). Equations. (12), and (13) are linear singular integral equations with Cauchy-type kernel. The theory of such equations is well elaborated,[23] and hence we can find a, b, and $J_1(x)$ for any given H_a.

To do this, we introduce the following notations:

$$\alpha\equiv\frac{1}{\pi}\arctan\frac{\gamma}{2}, \quad \beta\equiv\frac{1}{2}-\alpha,$$

$$\alpha_+\equiv\alpha, \quad \alpha_-\equiv\alpha+1,$$

$$F_\pm(t)\equiv(a^2-t^2)^{\alpha_\pm}|t^2-b^2|^\beta$$

and define the function $f(t)$ by the equalities

$$f(t)=-2H_0(t), \quad 0\leqslant t<b,$$

$$f(t)=2\sin\pi\alpha\cdot[H_z^0-H_0(t)], \quad b<t\leqslant a,$$

i.e., $f(t)$ is discontinuous at $t=b$. Then, the solution of Eqs. (12), and (13) can be represented as follows: In the interval $0\leqslant x^2\leqslant b^2$ one has

$$J_1(x)=\frac{2}{\pi}|x|F_\pm(x)\int_0^a\frac{f(t)dt}{(t^2-x^2)F_\pm(t)}, \tag{15}$$

while in the interval $b^2\leqslant x^2\leqslant a^2$ we arrive at

$$J_1(x)=\cos\pi\alpha\left[f(x)+\frac{\gamma}{\pi}|x|F_\pm(x)\int_0^a\frac{f(t)dt}{(t^2-x^2)F_\pm(t)}\right], \tag{16}$$

and $J_1(x)=0$ for $a^2\leqslant x^2\leqslant w^2$. Here the integrals are taken in the sense of the Cauchy principal value; F_+ and F_- refer to positive and negative values of γ, respectively. If $\gamma<0$, for the above solution to exist it is necessary that

$$\int_0^a\frac{f(t)}{F_-(t)}dt=0, \tag{17}$$

and

$$\int_0^a\frac{t^2f(t)}{F_-(t)}dt=0. \tag{18}$$

These two equalities enable us to determine b and a when $\gamma<0$. If $\gamma>0$, the necessary condition for the existence of the solution is

$$\int_0^a\frac{f(t)}{F_+(t)}dt=0. \tag{19}$$

A second relation between a and b in this case is obtained from the analysis of the magnetic field near the point $x^2=a^2$. It turns out that

$$H_z(x)-H_z^0\approx C_\pm\frac{\gamma}{2|\gamma|}(4+\gamma^2)^{1/2}(x^2-a^2)^{\alpha_\pm} \tag{20}$$

if x^2 tends to a^2 from above, and

$$H_z(x)-H_z^0\approx C_\pm(a^2-x^2)^{\alpha_\pm} \tag{21}$$

if x^2 approaches a^2 from below. Here $C_\pm$ are certain integrals independent of x; the subscripts $+$ and $-$ refer to the cases of positive and negative γ, respectively. Since $H_z(x)\geqslant H_z^0$ when $x^2>a^2$, we find that $C_+\geqslant 0$. On the other hand, one has $H_z(x)\leqslant H_z^0$ when $x^2<a^2$, and thus $C_\pm\leqslant 0$. Hence one concludes that $C_+=0$. This is the second equality in the case of positive γ, and it has the form

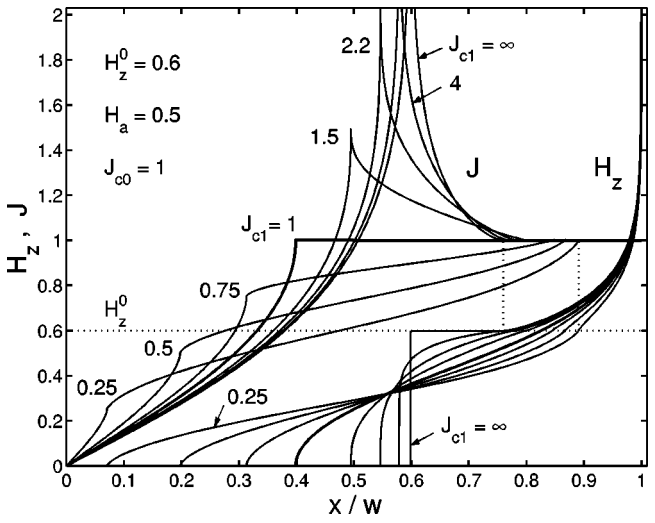

FIG. 2. Some profiles of the sheet current $J(x)$ and of the perpendicular magnetic field $H_z(x)$ in a superconductor thin strip with width $2w$ for various $J_c(H_z)$ dependences, Eq. (4), equivalent to various out-of-plane anisotropies, Eq. (5), in an applied field $H_a = 0.5$. The unit for both J and H is $J_{c0}=1$. The anisotropy parameters are $H_z^0=0.6$ and $J_{c1}=0.25$, 0.5, 0.75, 1, 1.5, 2.2, 4, and ∞. The isotropic (or Bean) case $J_{c1}=1$ is shown as bold lines. The dotted lines indicate the field $H_z=H_z^0$ and the position $x=a$, where $J(a)=J_{c0}$ and $H_z(a)=H_z^0$. In the limit $J_{c1}\to\infty$ the field $H_z(x)$ at the flux front $x=b$ abruptly jumps to the value H_z^0 and stays constant for $b\leqslant x\leqslant a$.

$$\int_0^b \frac{f(t)dt}{(a^2-t^2)F_+(t)} - \frac{f(a)}{2\alpha a(a^2-b^2)^{1/2}} + \int_b^a \left[\frac{f(t)}{t(t^2-b^2)^{\beta}} - \frac{f(a)}{a(a^2-b^2)^{\beta}}\right]\frac{tdt}{(a^2-t^2)^{1+\alpha}} = 0. \quad (22)$$

Equations. (19) and (22) determine a and b when $\gamma>0$.

III. ANALYSIS

Let us now analyze the obtained solution. For evaluation of the integrals in Eqs. (9), (15)–(19), and (22) we use the method given in the Appendix. Some profiles $J(x)$, Eq. (6), and $H_z(x)$, Eq. (9), obtained in this way are shown in Figs. 2 to 5. On examination of these results as well as of the subsequent formulas it is useful to keep in mind the following: The case $\gamma>0$ corresponds to the peak in $j_c(\theta)$ at $\theta=\pi/2$; the relative height of the peak is specified by the parameter J_{c1}/J_{c0}, while its width is determined by H_z^0, $\tan[(\pi/2)-\theta_0]=2H_z^0/J_{c0}$. Thus the higher and narrower is the peak in $j_c(\theta)$, the larger is our parameter $\gamma=(J_{c1}-J_{c0})/H_z^0$. As opposed to this, a peak at $\theta=0$ results in $\gamma<0$; the width of this peak decreases with increasing parameter H_z^0, $\tan\theta_0=J_{c0}/2H_z^0$, and its relative height is proportional to J_{c0}/J_{c1}.

It should be noted here that no restriction on C_- is obtained when $\gamma<0$. In this situation the constant C_- is not equal to zero but negative, and thus the derivative of H_z with respect to x becomes infinite at $x=a$. In the same point a sharp bend occurs in $J(x)$. In other words, we obtain that *two* flux fronts exist in the sample, at $x=b$ and at $x=a$, see

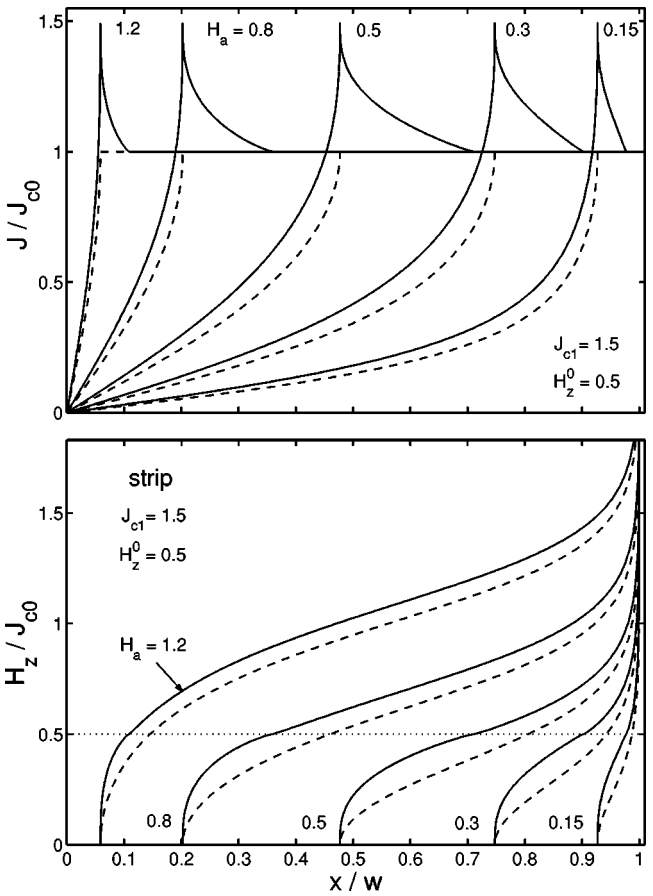

FIG. 3. Profiles of the sheet current $J(x)$ (top) and of the magnetic field $H_z(x)$ in a thin strip with width $2w$ and anisotropic pinning (solid lines) in an increasing applied field $H_a=0.15$, 0.3, 0.5, 0.8, and 1.2 in units of $J_{c0}=1$. The anisotropy parameters are $J_{c1}/J_{c0}=1.5$ and $H_z^0/J_{c0}=0.5$, thus $\gamma=1$. The dashed lines show the profiles of an isotropic strip for the same values of the front position $b_0(H_a)$, Eq. (28). Note the sharp peak of $J(x)$ at $x=b$ of height $J(b)=J_{c1}$ and the steep front of $H_z(x)$ at $x=b$ for this type of anisotropy. At $x=a$, $J(x)$ reaches the value $J_{c0}=1$ and $H_z(x)$ goes through the value $H_z(a)=H_z^0$ marked by a dotted line.

Figs. 2, 4, and 5. Of course, the singularities in H_z and in J at $x=a$ result from the sharp bend in our model $J_c(H_z)$ at $H_z=H_z^0$, see Eqs. (4) and Fig. 1. However, one may expect that in the case $\gamma<0$ our qualitative conclusion on the existence of the second flux front in the sample remains valid if $J_c(H_z)$ is a smooth function but its behavior changes abruptly over an interval smaller than H_{cs}. Such changes indeed may occur if the critical current density has sufficiently sharp angular dependence $j_c(\theta)$.

We shall now describe $H_z(x)$ and $J(x)$ in the vicinity of the point $x=b$ in which $H_z=0$. According to Eq. (14), at this point $|J(b)|=J_{c1}$. When $x^2\leqslant b^2$, it follows from the exact solution that

$$|J(x)|-J_{c1}\approx C_b^{\pm}(b^2-x^2)^{\beta}, \quad (23)$$

while if $x^2\geqslant b^2$, one has

$$|J(x)|-J_{c1}\approx \frac{\gamma}{(4+\gamma^2)^{1/2}} C_b^{\pm}(x^2-b^2)^{\beta}. \quad (24)$$

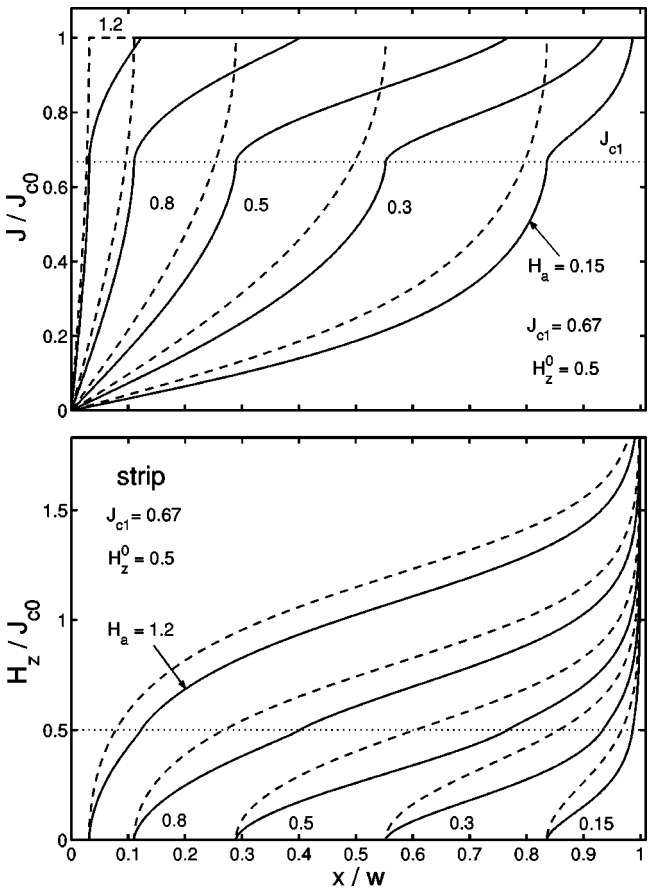

FIG. 4. As Fig. 3, but for different type of anisotropy, $J_{c1}/J_{c0}=0.67$ and $H_z^0/J_{c0}=0.5$, thus $\gamma=-0.67$. In this case $J(x)$ is monotonic and has an inflection point with vertical slope at $x=b$ where $J(b)=J_{c1}$ (dotted line). The penetrating front of $H_z(x)$ is now less steep than in the isotropic case, which is shown as dashed lines.

Here C_b^+ and C_b^- are certain integrals which do not depend on x and have negative values. Formulas (23) and (24) show that in the case $\gamma>0$, $|J(x)|$ has a sharp peak at $x=b$, whereas for $\gamma<0$, $J(x)$ is a monotonic function and its derivative with respect to x becomes infinite at $x=b$, see Figs. 2, 4, and 5. Taking into account the above formulas and Eq. (14), one obtains the distribution of H_z near $x=b$,

$$H_z=0 \quad \text{for} \quad x\leqslant b, \tag{25}$$

$$H_z=-\frac{C_b^{\pm}}{(4+\gamma^2)^{1/2}}(x^2-b^2)^{\beta} \quad \text{for} \quad x\geqslant b. \tag{26}$$

When $\gamma=0$, we arrive at the well-known result[4,20,21] $H_z^0 \propto (x^2-b^2)^{1/2}$. However, in the general case, taking into account the equality $\beta=\frac{1}{2}-(1/\pi)\arctan(\gamma/2)$, one may conclude that the greater γ is, the sharper is the H_z profile, Fig. 2. Interestingly, the dependence $(x-b)^{\beta}$ sufficiently well describes $H_z(x)$ even if x is not too close to b, see Fig. 6.

Consider now the solution in the limit of small positive values of γ. If $\gamma\to 0$, two cases are possible: H_z^0 remains a constant, or it increases as γ^{-1} (i.e., $J_{c1}-J_{c0}=\text{const}$). In the first case one has $\alpha\approx\gamma/2\pi$, $H_a-H_b\propto\gamma$, and the function $f(t)$ tends to zero. Thus, according to Eqs. (15) and (16), $J_1\to 0$, and the solution goes over to the well-known

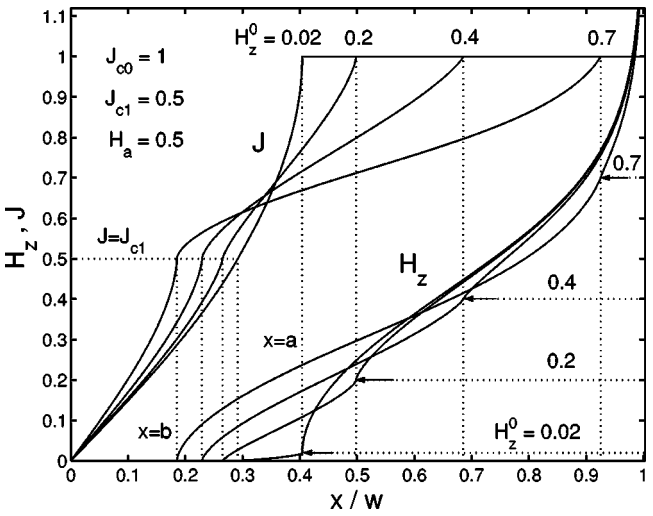

FIG. 5. Profiles of $J(x)$ (left) and $H_z(x)$ (right) in a thin strip with anisotropic pinning of the type $J_{c1}=0.5$ for various values of $H_z^0=0.02,0.2,0.4$, and 0.7 in a constant applied field $H_a=0.5$ (in units of $J_{c0}=1$). The dotted lines at $x=b$, $x=a$, $J=J_{c1}$, and $H_z=H_z^0$ shall help to identify the features $J(b)=J_{c1}$, $J(a)=J_{c0}$, and $H_z(a)=H_z^0$. Note that with decreasing H_z^0 the penetrating flux front at $x=b$ becomes less pronounced and a new front appears at $x=a$. In the limit $H_z^0\to 0$ only the front at $x=a$ remains and the profiles look like in the isotropic strip with b replaced by a.

result[4,20,21] for the Bean critical state model with $J_c=J_{c0}$. In the second case $J_0(x)+J_1(x)$ also tends to the solution corresponding to a constant J_c but now $J_c=J_{c1}$.

In the limiting case $\gamma\to+\infty$, this parameter drops out from Eqs. (15), (16), (19), and (22), and $J_1(x)$ depends only on H_z^0, J_{c0}. In other words, if $J_{c1}\gg J_{c0}, H_z^0$ or $J_{c1}>J_{c0}\gg H_z^0$, the solution becomes practically independent of J_{c1}. The distribution of the magnetic field in this case can be understood using Eq. (26). It turns out that $C_b^+\approx-\gamma H_z^0$ for $\gamma\gg 1$, and hence

$$H_z(x)\approx H_z^0(x^2-b^2)^{\beta} \tag{27}$$

with $\beta\to 0$. This means we have an abrupt step of height H_z^0 at $x=b$ (see Fig. 2).

It should be emphasized that this limiting case, $\gamma\to+\infty$, corresponds to intrinsic pinning in high-T_c superconductors in which the ratio $[j_c(\pi/2)/j_c(0)]=J_{c1}/J_{c0}$ can be sufficiently large (see, e.g., Ref. 24). Thus our solution of this limit can be used for analyzing the critical state in these superconductors. As has already been mentioned above, a characteristic feature of this case is the extreme steepness of the $H_z(x)$ profile in the vicinity of the point $x=b$. Besides this, it follows from Eqs. (19) and (22) that the position of the flux front, b/w, is a function only of H_a/H_{cs} and of the parameter H_z^0/H_{cs}, see Fig. 7. In general this function *cannot* be fitted by scaling the dependence found in the isotropic case,[4]

$$\frac{b_0}{w}=\frac{1}{\cosh(H_a/H_{cs})}, \tag{28}$$

using some effective value of H_{cs}. Rather, the shape of $b(H_a)$ essentially depends on the ratio H_z^0/H_{cs}. Therefore

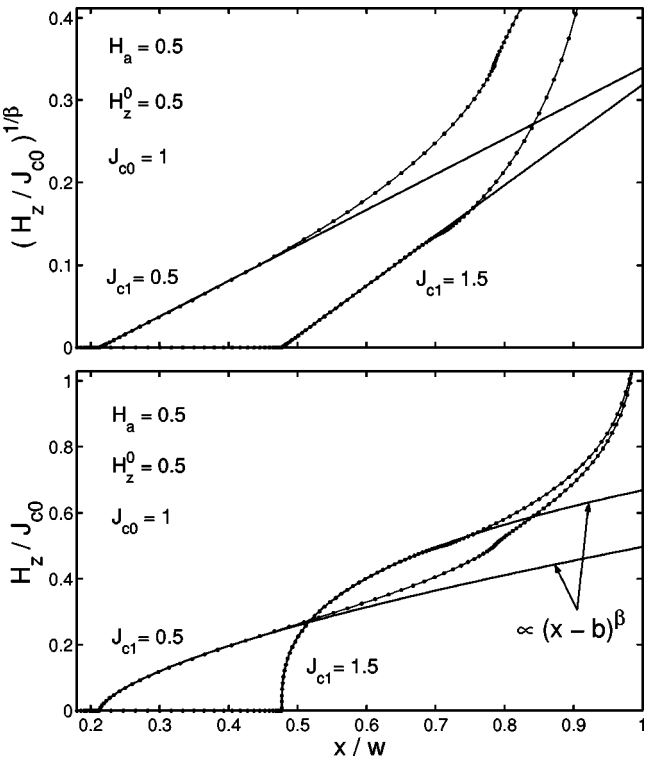

FIG. 6. Comparison of the shape of the profile $H_z(x)$ near the flux front with the expression $(x-b)^{\beta}$ suggested by Eq. (26). Shown are examples with $H_a=0.5$ (in units of $J_{c0}=1$) and two different anisotropies: $H_z^0=0.5$, $J_{c1}=1.5$ (thus $\gamma=1$, $\alpha=0.148$, $\beta=0.352$, $b=0.477$, $a=0.711$) and $H_z^0=0.5$, $J_{c1}=0.5$ (thus $\gamma=-1$, $\alpha=-0.148$, $\beta=0.648$, $b=0.213$, $a=0.784$). The exact $H_z(x)$ (dotted lines) is well fitted over a large interval of x by the function $c\cdot(x-b)^{\beta}$ (solid lines) with $c=0.840$ or $c=0.580$ for these two examples (with x and b in units of the strip half width w). The solid lines in the upper plot are straight lines fitting $H_z(x)^{1/\beta}$.

measuring $b(H_a)$ in principle can give information not only on $H_{cs}=J_{c0}/\pi$ but also on H_z^0, i.e., about the width of the peak in $j_c(\theta)$, see Eq. (5). In particular, when $H_z^0 \ll J_{c0}$, Eqs. (19) and (22) lead to the following expression for the front position:

$$\left(\frac{b}{w}\right)^2 \approx \frac{1+k\cdot(H_z^0/H_{cs})^2\tanh^2(H_a/H_{cs})}{\cosh^2(H_a/H_{cs})}, \qquad (29)$$

where the constant k is determined by the root of the equation

$$\frac{\pi}{4}(u^2-1)=u-\arctan u,$$

$$k=\frac{16}{\pi^2}\frac{u^2}{(1+u^2)^2}\approx 0.394.$$

Note that the right-hand side of Eq. (29) cannot be reduced to the dependence (28) in the whole interval of changes of H_a when H_z^0 is different from zero. The exact values of the front position $b(H_a)$ are shown in Fig. 7 for the limit of large $\gamma \gg 1$, for $J_{c1}=11$ and $H_z^0=0\cdots 1.5$ in units of $J_{c0}=1$.

In the third limiting case when $\gamma\to-\infty$, one has $\beta\to 1$, $C_b^-\sim -H_z^0$ and the induction profile becomes

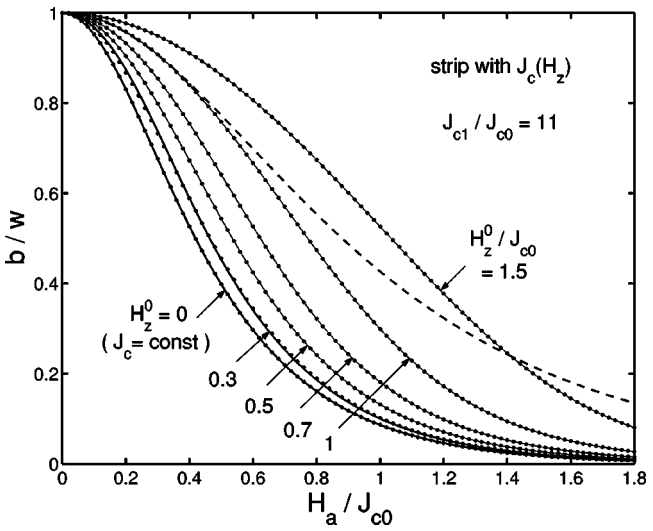

FIG. 7. The position b of the flux front, or penetration depth $w-b$, of a superconductor thin strip with width $2w$ and various $J_c(H_z)$ dependences, Eq. (4), plotted versus the applied magnetic field H_a in units of $J_{c0}=1$. The dotted lines are computed as described in Sec. III for anisotropy parameters $J_{c1}=11$ and $H_z^0=0$, 0.3, 0.5, 0.7, 1, and 1.5. The bold solid lines for $H_z^0=0$ and 0.3 are from Eq. (29) and fit the exact data very well. The dashed line $b/w=1/\cosh[H_a/(2.1H_{cs})]$, obtained by stretching the isotropic ($J_c=\text{const}$) expression, Eq. (28), by a factor of 2.1, demonstrates that such scaling of the isotropic result cannot fit the anisotropic result.

$$H_z(x)\propto(x^2-b^2) \qquad (30)$$

with a small prefactor of the order of $H_z^0/|\gamma|$. Thus for $-\gamma \gg 1$ the flux front at $x=b$ practically disappears while, according to Eq. (20), the second front near $x=a$ is well developed, see Fig. 5.

Finally, we consider in some detail the case of small negative values of γ when $H_z^0 \gg H_{cs}=J_{c0}/\pi$ while the ratio J_{c0}/J_{c1} is not close to unity. This case can give some idea of pinning by columnar defects, which produce a peak in $j_c(\theta)$ at $\theta=0$. Indeed, if one assumes that the characteristic width of the peak, θ_0, is small ($\theta_0 \ll 1$), then it follows from the definitions of H_z^0 and γ that $H_z^0 \approx J_{c0}/2\theta_0$ and $|\gamma|<2\theta_0$. Since the solution with $\gamma=0$ and $J_c=J_{c1}$ describes the critical state in the strip before the irradiation [we assume that the columnar defects do not change $j_c(\theta)$ at $\theta>\theta_0$], the difference between the solutions corresponding to $\gamma\neq 0$ and $\gamma=0$ provides information on pinning by columnar defects. In the considered case this difference is small, and it can be analyzed analytically. As a result of the analysis, we conclude that after the irradiation the current and H_z profiles remain practically unchanged in most of the sample except for narrow regions near its edges where H_z becomes large. In these regions J increases up to J_{c0}. The increase of the current diminishes the penetration depth, and we obtain the following relation between the positions of the flux fronts, b and b_1, obtained at the same H_a in the strip with and without columnar defects, respectively:

$$\operatorname{arccosh}\frac{w}{b_1}-\operatorname{arccosh}\frac{w}{b}=\frac{|\gamma|}{\pi}g(h), \qquad (31)$$

where $h \equiv \pi H_a / J_{c1}$, $w/b_1 = \cosh(h)$, and the function $g(h)$ has the form

$$g(h) = \int_0^h \ln(2\cosh t)\, dt. \tag{32}$$

Since g is a nonlinear function of h,

$$g(h) \approx \frac{1}{2}h^2 + 0.411(1 - e^{-1.8h}), \tag{33}$$

the exact dependence $b(H_a)$ cannot be described by Eq. (28) with some effective H_{cs}. The prefactor

$$\frac{|\gamma|}{\pi} \approx \frac{2\theta_0}{\pi} \frac{j_c(0) - j_c(\pi/2)}{j_c(0)}$$

in Eq. (31) is determined by the characteristics of pinning by the columnar defects, i.e., by the width and height of the peak in $j_c(\theta)$.

IV. CONCLUSIONS

An exact solution of the critical state equations for the strip in perpendicular magnetic field is derived for an induction-dependent critical sheet current $J_c(H_z)$ described by Eqs. (4). This simple model dependence may be used to simulate the intrinsic pinning by CuO planes ($\gamma > 0$) or pinning by extended defects ($\gamma < 0$) in high-T_c superconductors. In the case $\gamma > 0$, the H_z profile in the vicinity of the flux front is sharper than in the isotropic case, and the current density has a sharp peak there. In the limiting case, $\gamma \gg 1$, which may describe the intrinsic pinning in high-T_c superconductors, the field profile $H_z(x)$ has a sharp rectangular step. In the opposite situation, $\gamma < 0$, *two flux fronts* can occur in the superconductor; the H_z profile near $x = b$ is less steep than in the isotropic case, and the current density is a monotonic function of x. In both cases of positive and negative γ the profile $H_z(x)$ in a sufficiently large vicinity of the flux front is well approximated by the expression $H_z(x) \approx (x-b)^{\beta}$ with the exponent $\beta = 0.5 - \pi^{-1}\arctan(\gamma/2)$.

In high-T_c superconductors the penetration and distribution of magnetic flux over the sample can be determined with high spatial resolution using magneto-optical techniques[25] or microscopic Hall-sensor arrays.[26] The data of Figs. 6, and 7 and Eq. (31) clearly show that the experimental investigation of flux-density profiles near the flux front and of the H_z dependence of the penetration depth can give information not only on the strength but also on the *anisotropy* of flux-line pinning in superconductors. Our analytical solution, though derived for a simplified model, allows one to estimate the characteristic width and height of peaks in the out-of-plane anisotropic pinning strength $j_c(\theta)$.

ACKNOWLEDGMENTS

G.P.M. acknowledges the hospitality of the Max-Planck-Institut für Metallforschung, Stuttgart.

APPENDIX: NUMERICAL EVALUATION

The condition that two integrals have to vanish, e.g., Eqs. (17) and (18) of the form $I_1(a,b) = 0$ and $I_2(a,b) = 0$, we satisfy by minimizing the function $U(a,b) = I_1^2 + I_2^2$ with respect to a and b. After this we calculate the sheet current $J_1(x)$ from Eqs. (15) and (16) and the magnetic field $H_z(x)$ from Eqs. (9) and (14).

The integrals (9), (15)–(19), and (22) over the variable t have integrands which possess one or several infinities at the points $t = 0$, $t = x$, $t = b$, and $t = a$ where the denominators vanish. We evaluate such integrals in the following way.

In the integrals containing a factor $(t-x)^{-1}$ we subtract the singular part and integrate it analytically, e.g.,

$$\int_0^a \frac{f(t)\,dt}{t^2 - x^2} = \int_0^a \frac{f(t) - f(x)}{t^2 - x^2}\, dt - \frac{f(x)}{2x} \ln\frac{a+x}{a-x}. \tag{A1}$$

Then we divide the integration interval into pieces bounded by the remaining singularities, $0 \leqslant t \leqslant b$, $b \leqslant t \leqslant a$, and $a \leqslant t \leqslant 1$. In each interval we substitute the integration variable by an appropriate function $t = t(u)$ and integrate over u such that the new integrand has no infinity and vanishes rapidly at the boundaries. This new integral may thus be evaluated as a sum over an equidistant grid u_i with constant weights. For example we write

$$\int_0^{\tau} g(t)\,dt = \int_0^1 g[t(u)]\, t'(u)\, du \approx \sum_{i=1}^{N} g_i w_i \tag{A2}$$

with $g_i = g[t(u_i)]$, $u_i = (i - 1/2)/N$, $w_i = t'(u_i)/N$, $t'(u) = dt/du$, and $i = 1,2,3,\ldots N$. This integration method is very accurate if the substitution is chosen such that the weights w_i and the products $g_i w_i$ vanish rapidly at the integration boundaries, e.g., $w_i \sim u_i^p$ and $w_i \sim (1-u_i)^q$ with $p \gg 1$ and $q \gg 1$. Simple choices of this substitution in the example (A2) are

$$t(u) = (3u^2 - 2u^3)\tau, \quad t'(u) = 6u(1-u)\tau, \tag{A3}$$

or better,

$$t(u) = (10u^3 - 15u^4 + 6u^5)\tau, \quad t'(u) = 30u^2(1-u)^2\tau. \tag{A4}$$

Higher accuracy is achieved by the following substitution. We chose equidistant $u_i = (i - 1/2)/N$ as above and then iterate Eq (A3) m times starting with $s_i = u_i$ and $w_i = \tau/N$ according to

$$w := 6(s - s^2)w, \quad s := 3s^2 - 2s^3 \quad (m \text{ times}). \tag{A5}$$

Finally we write $t(u_i) = s_i \tau$. The weights $w_i = t'(u_i)/N$ of this substitution vanish at the boundaries with exponents $p = q = 2^{(m-1)}$, which can be made arbitrarily large. For example, using $m = 5$ iterations one gets the exponents $p = q = 2^4 = 16$.

An infinity $g(t) \propto 1/t^{\eta}$ in the original integral (A2) leads, after this substitution, to a new integrand vanishing at $t = 0$ as $g[t(u)]t'(u) \propto u^{\vartheta}$ with $\vartheta = p(1-\eta) - \eta$. Thus for the example $\eta = 1/2$ with $p = 16$ the new integrand near $u = 0$ vanishes as $u^{7.5}$ and the terms in the sum (A2) as $(i - 1/2)^{7.5}$, in spite of the singular original integrand. For general exponent η, to reach high accuracy one should choose m so large that the new exponent is $\vartheta = (1-\eta)2^{m-1} - \eta \geqslant 4$, or approxi-

mately $m \geqslant 3.5 - 1.5\ln(1-\eta)$. To avoid spurious results due to rounding errors, one has to add in all vanishing denominators a small $\epsilon \approx 10^{-15}$ by writing, e.g., $(|t^2-b^2|+\epsilon)^{\beta}$.

In the limit of a large negative slope $\gamma \to -\infty$ one has $\beta \to 1$ and the integrals (17) and (18) containing a factor $|t^2-b^2|^{-\beta}$ are close to diverging. In this case the singular part in these integrals should be integrated analytically, similar as shown in Eq. (A1). The subtracted terms are conveniently chosen such that the integral which has to be taken analytically is simple, e.g., $\int t \cdot (b^2-t^2)^{-\beta} dt$. Note that the numerator $f(t)$ in Eqs. (15)–(19) and (22) is discontinuous at $t=b$.

[1] C.P. Bean, Phys. Rev. Lett. **8**, 250 (1962); Rev. Mod. Phys. **36**, 31 (1964).
[2] A.M. Campbell and J.E. Evetts, Adv. Phys. **72**, 199 (1972).
[3] P.N. Mikheenko and Yu.E. Kuzovlev, Physica C **204**, 229 (1993).
[4] E.H. Brandt, M. Indenbom, and A. Forkl, Europhys. Lett. **22**, 735 (1993).
[5] W.T. Norris, J. Phys. D **3**, 489 (1970).
[6] G.P. Mikitik and E.H. Brandt, Phys. Rev. B **60**, 592 (1999).
[7] E.H. Brandt, Phys. Rev. B **54**, 4246 (1996).
[8] E.H. Brandt, Phys. Rev. B **58**, 6506 (1998); **58**, 6523 (1998).
[9] Y.B. Kim, C.F. Hempstead, and A. Strnad, Phys. Rev. **129**, 528 (1963).
[10] S. Senoussi, J. Phys. III **2**, 1041 (1992).
[11] E.H. Brandt, Rep. Prog. Phys. **58**, 1465 (1995).
[12] J. McDonald and J.R. Clem, Phys. Rev. B **53**, 8643 (1996).
[13] D.V. Shantsev, Y.M. Galperin, and T.H. Johansen, Phys. Rev. B **60**, 13 112 (1999).
[14] E.H. Brandt, Physica C **235-240**, 2939 (1994).
[15] I.M. Babich and G.P. Mikitik, Phys. Rev. B **54**, 6576 (1996).
[16] I.M. Babich and G.P. Mikitik, Pis'ma Zh. Éksp. Teor. Fiz. **64**, 538 (1996) [JETP Lett. **64**, 586 (1996)];
[17] I.M. Babich and G.P. Mikitik, Phys. Rev. B **58**, 14 207 (1998).
[18] G. P. Mikitik and E. H. Brandt, preceding paper, Phys. Rev. B **62**, 6800 (2000).
[19] E. Zeldov, A.I. Larkin, V.B. Geshkenbein, M. Konczykowski, D. Majer, B. Khaykovich, V.M. Vinokur, and H. Shtrikman, Phys. Rev. Lett. **73**, 1428 (1994); M.V. Indenbom and E.H. Brandt, *ibid.* **73**, 1731 (1994); I.L. Maksimov and A.A. Elistratov, Pis'ma Zh. Éksp. Teor. Fiz. **61**, 204 (1995) [JETP Lett. **61**, 208 (1995)]; N. Morozov, E. Zeldov, D. Majer, and B. Khaykovich, Phys. Rev. Lett. **76**, 138 (1996); M. Benkraouda and J.R. Clem, Phys. Rev. B **53**, 5716 (1996); **58**, 15 103 (1998); C.J. van der Beek, M.V. Indenbom, G. D'Anna, and W. Benoit, Physica C **258**, 105 (1996); R. Labusch and T.B. Doyle, *ibid.* **290**, 143 (1997); T.B. Doyle, R. Labusch, and R.A. Doyle, *ibid.* **290**, 148 (1997); E.H. Brandt, Phys. Rev. B **59**, 3369 (1999); **60**, 11 939 (1999).
[20] E.H. Brandt and M.V. Indenbom, Phys. Rev. B **48**, 12 893 (1993).
[21] E. Zeldov, J.R. Clem, M. McElfresh, and M. Darwin, Phys. Rev. B **49**, 9802 (1994).
[22] M. Tachiki and S. Takahashi, Solid State Commun. **70**, 291 (1989).
[23] N. Muskhelishvili, *Singular Integral Equations* (Nordhoff, Groningen, Holland, 1953).
[24] B. Roas, L. Schultz, and G. Saemann-Ischenko, Phys. Rev. Lett. **64**, 479 (1990).
[25] L.A. Dorosinskii, M.V. Indenbom, V.I. Nikitenko, Yu.A. Ossip'yan, A.A. Polyanskii, and V.K. Vlasko-Vlasov, Physica C **203**, 149 (1992); T. Schuster, M.V. Indenbom, H. Kuhn, E.H. Brandt, and M. Konczykowski, Phys. Rev. Lett. **73**, 1424 (1994).
[26] E. Zeldov, A.I. Larkin, V.B. Geshkenbein, M. Konczykowski, D. Majer, B. Khaykovich, V.M. Vinokur, and H. Shtrikman, Phys. Rev. Lett. **73**, 1428 (1994); W. Xing, B. Heinrich, Hu Zhou, A.A. Fife, and A.R. Cragg, J. Appl. Phys. **76**, 4244 (1994).